NASA TECHNICAL MEMORANDUM

NASA TM X-1511

NASA TM X-1511

COMBUSTION INSTABILITY IN STEEL AND ABLATIVE ROCKET CHAMBERS

by Ralph R. Goelz

Lewis Research Center
Cleveland, Ohio

NATIONAL AERONAUTICS AND SPACE ADMINISTRATION • WASHINGTON, D. C. • FEBRUARY 1968

NASA TM X-1511

COMBUSTION INSTABILITY IN STEEL AND ABLATIVE ROCKET CHAMBERS

By Ralph R. Goelz

Lewis Research Center
Cleveland, Ohio

NATIONAL AERONAUTICS AND SPACE ADMINISTRATION

For sale by the Clearinghouse for Federal Scientific and Technical Information
Springfield, Virginia 22151 – CFSTI price $3.00

COMBUSTION INSTABILITY IN STEEL AND ABLATIVE ROCKET CHAMBERS

by Ralph R. Goelz

Lewis Research Center

SUMMARY

An investigation was conducted at the Lewis Research Center to compare the effects of ablative chambers and steel chambers on combustion instability in a hydrogen-oxygen rocket engine. Both uncharred and charred ablative materials were evaluated. Two concentric tube injectors were used for the testing at a chamber pressure of 300 psia (2070 kN/m^2) and a nominal thrust of 20 000 pounds (89 kN). Hydrogen-injection temperature ramping was the basic stability rating technique. In addition, an instability amplitude comparison analysis was completed to detect amplitude variations for the two materials.

Both techniques, the hydrogen-injection temperature ramping and the amplitude analysis lead to the same conclusion: There is no significant difference in stability limit or instability amplitude between the steel, charred ablative, and uncharred ablative chambers.

INTRODUCTION

For development programs of large injectors, it is desirable to have combustion chambers less expensive than the cooled steel type. Ablative chambers offer a logical alternative. For example, the M-1 hydrogen-oxygen injector with 1 500 000-pound (6670-kN) nominal vacuum thrust was stability rated in an ablative chamber (ref. 1). The question arose whether the ablative chamber stability data would be representative of the final metal configuration. No published information was found concerning this material effect, although unpublished data in the Apollo Program indicated that ablative material has a stabilizing effect. Consequently, a short test program with 20 000-pound (89-kN) hydrogen-oxygen engines was devised to obtain (1) minimum stable hydrogen-injection temperature comparisons, and (2) amplitude comparisons during instability.

APPARATUS

Test Facility

The Rocket Engine Test Facility (fig. 1) at Lewis is a 50 000-pound (222-kN) thrust stand equipped with an exhaust gas muffler and scrubber. The rocket engine was mounted on the thrust stand to fire vertically into the scrubber where the exhaust gases were sprayed with water for cooling and sound suppression.

The facility used pressurized propellant tanks to flow the propellants from the propellant tanks to the engine. The oxygen propellant pipeline was immersed in a nitrogen bath. The liquid-hydrogen pipeline was insulated with a vacuum jacket.

The facility was operated remotely from a control room located 2000 feet (610 m) from the test stand. The control room was equipped with several oscillographs to record temperature and pressure data. High-frequency pressure oscillation data were recorded on magnetic tape. Additional facility and instrumentation information is available in reference 2.

Injector and Engine

Two injectors used for this evaluation were of identical design and had 487 concen-

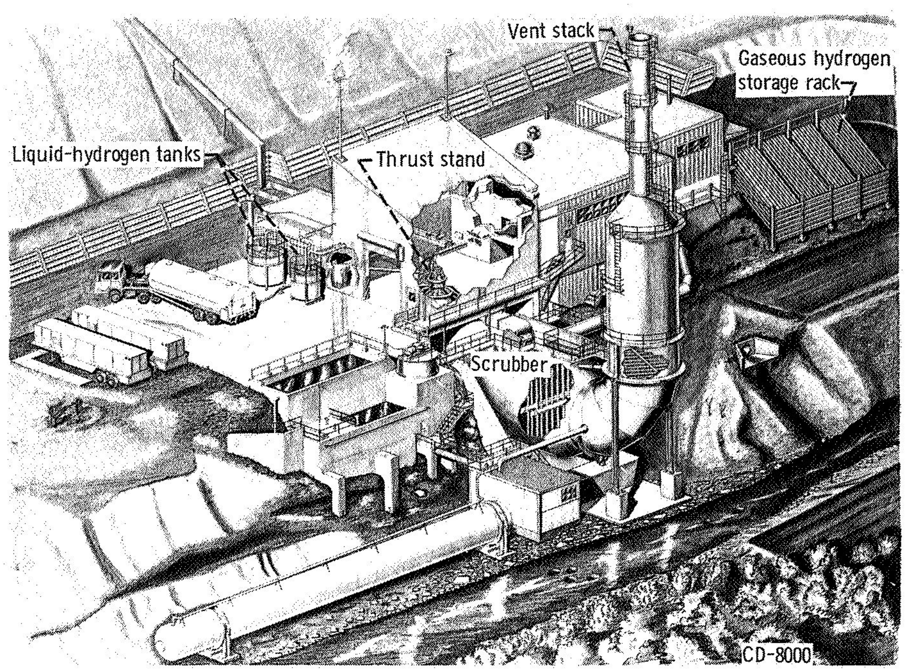

Figure 1. - Rocket engine test facility.

tric tube elements. The injectors were transpiration cooled and had an element injection-area ratio A_{H_2}/A_{O_2} of 2.52. One injector face burned through after being exposed to 5-seconds of combustion instability. A replacement injector was required to finish the test series.

The steel cylindrical heat-sink thrust chamber was 10.77 inches (27.4 cm) inside diameter including a 0.03-inch (0.76-mm) thick flame-sprayed zirconium oxide coating. The inside chamber diameter of the two ablative configurations (uncharred and charred) was nominally 10.77 inches (27.4 cm). Shown in figure 2 is the ablative chamber mounted on the thrust stand. cross sections of the chambers used are shown in figure 3. For all tests, the convergent-divergent exhaust nozzle had a contraction ratio of 1.90 and an expansion ratio of 1.30. Throughout most tests, the characteristic exhaust velocity efficiency was approximately 98.0 percent.

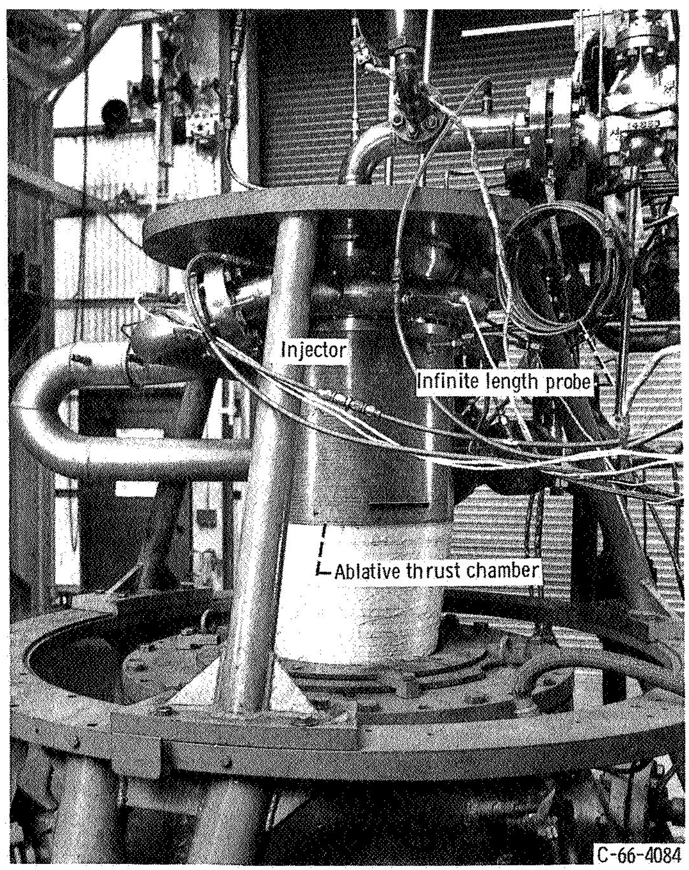

Figure 2. - Ablative chamber mounted on thrust stand.

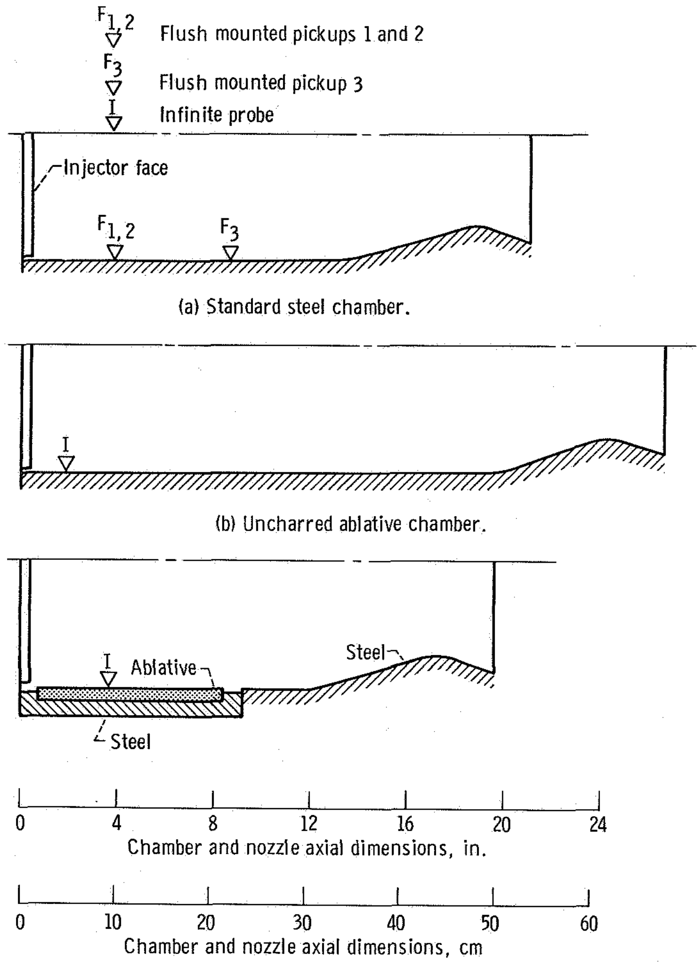

(c) Charred ablative chamber.

Figure 3. - Rocket engine cross sections showing axial locations of high-frequency pressure pickups.

Instrumentation

All low-frequency pressure measurements were made with strain-gage bridge transducers. The transducer nonlinearity or hysteresis did not exceed ±0. 5 percent of the full-scale output. The flow rate of liquid hydrogen was measured with a venturi, gaseous hydrogen with an orifice plate, and liquid oxygen with a vane flowmeter. Cryogenic temperatures were measured with carbon and platinum resistance probes that were accurate to $\pm 1^{\circ}$ R ($\pm 0.56^{\circ}$ K) in the measured range. Ambient temperatures were measured with iron-constantan thermocouples. All low-frequency signals were transmitted to the Lewis automatic digital data recording system.

High-frequency chamber pressure variations resulting from combustion instability were measured in the steel chambers with piezoelectric, water-cooled, flush-mounted transducers. The high-frequency signal was recorded on tape. The response of the piezoelectric transducers as installed was flat within 10 percent to a frequency of 6000 hertz with a resonant frequency of 20 000 hertz. One infinite length probe installed on the ablative chamber substituted for three flush-mounted transducers used during steel chamber tests. The infinite length probe was constructed from a length of tubing attached to the rocket chamber at one end and closed at the other. A piezoelectric transducer was installed approximately 5 inches (12.7 cm) from the chamber end of the tubing. Figure 2 shows the infinite length probe mounted on the chamber. Additional infinite length probe information can be found in reference 3. Because of the possibility of significant ablative chamber diameter change, the infinite length probe was selected to prevent possible damage to the flush-mounted transducers.

PROCEDURE

All configurations were stability rated by hydrogen-injection-temperature ramping. The hydrogen-injection-temperature ramp was accomplished by starting the run on a mixture of liquid hydrogen and ambient-temperature gaseous hydrogen. As the run progressed, the percentage of gas was reduced while simultaneously increasing the liquid-hydrogen flow to maintain constant total-hydrogen flow. Mixing was accomplished by swirling the liquid into the gaseous-hydrogen stream. Propellant flow rates were controlled with valves operated by electrohydraulic servosystems. The hydrogen-injection temperature at which the chamber-pressure oscillation amplitude suddenly became substantially greater than the normal noise level was defined as the transition temperature to instability. The testing was carried out in the following phases:

(1) The infinite probe was installed in a steel chamber with standard high-frequency pressure pickups for amplitude comparisons during combustion instability.

(2) Injectors 86 and 87 were stability rated in a steel chamber with a steel nozzle (fig. 3(a)) at various oxidant-fuel ratios.

(3) Injector 87 was stability rated in an uncharred ablative chamber with an ablative nozzle (fig. 3(b)) at various oxidant-fuel ratios.

(4) The ablative chamber was charred by a 17-second test including 5 seconds of instability.

(5) Injector 86 was stability rated in a chamber with a 7.5-inch (19.0-cm) insert of the previously charred ablative chamber and a steel nozzle (fig. 3(c)) at various oxidant-fuel ratios.

All tests, except the charring test were limited to an approximately 2.0-second duration, which was sufficient to obtain all necessary data. These short tests minimized material erosion between each test. The chamber pressures were nominally 300 psia (2070 kN/m^2) with oxidant-fuel ratios ranging from 3.5 to 6.0.

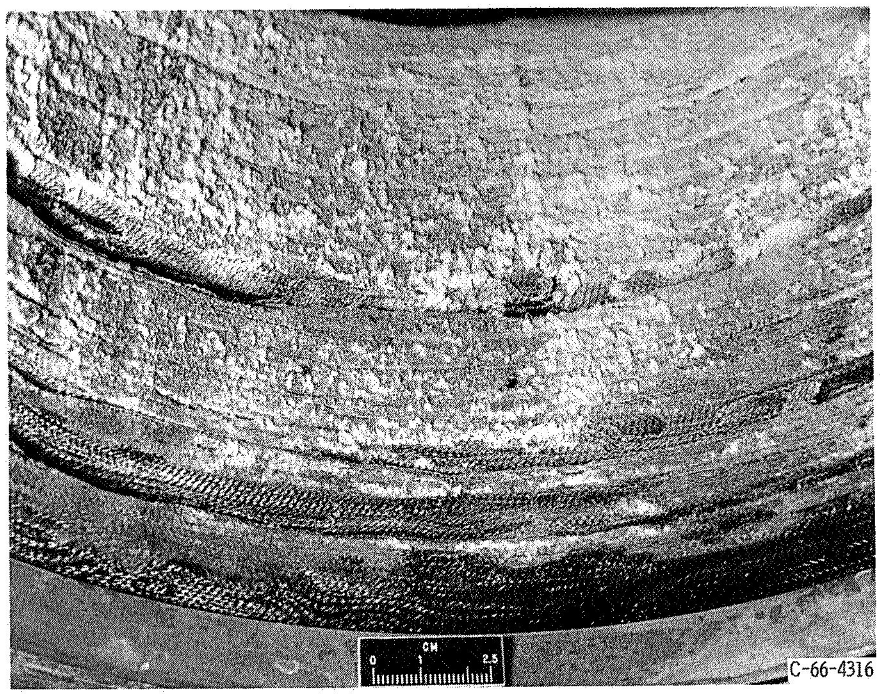

Figure 4. - Ablative material showing charred surface. Duration of run, 17 seconds.

The 17-second test charred the ablative material (fig. 4). The average char depth was 0.22 inch (5.58 mm) with an increase of 0.05 inch (1.27 mm) on the chamber diameter. The resulting silica surface roughness was approximately 0.06 inch (1.53 mm) peak to valley. At various locations, circumferential chunks of ablative were broken from the chamber wall. A hole was burned through the face plate of injector 87 during the charring test. Injector 86 was used for further testing.

RESULTS AND DISCUSSION

Instability Transition Temperature

Figure 5 summarizes the stability data which are also tabulated in table I. Injectors 86 and 87, which are identical in design have similar transition temperatures when tested with a steel chamber. It was thereby assumed that the injectors could be used interchangeably for the ablative stability rating tests. In table I, some of the injector 87 unstable hydrogen-injection temperature data are higher than the transition data. This discrepancy was the result of leading the engine start sequence with liquid-hydrogen propellant. Instability was initiated at the lower temperatures and could not be eliminated, although the temperature was subsequently increased to 10^{O} R (5.6^{O} K) above the

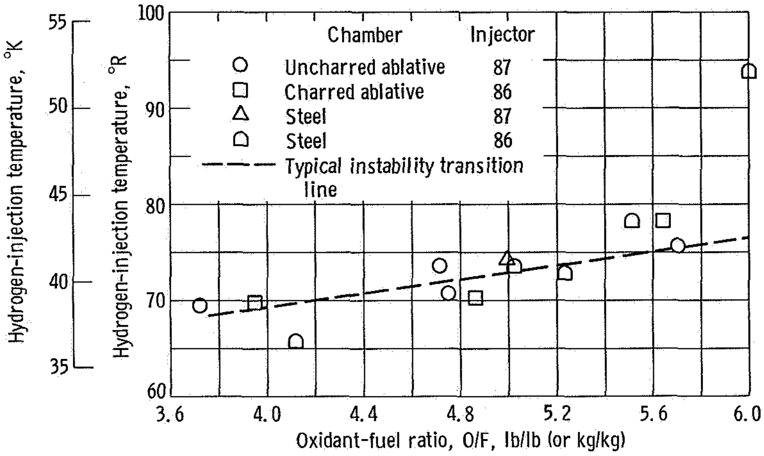

Figure 5. - Instability transition temperature.

transition. Other tests, including the work reported by Tomazic, et al. (ref. 1), have shown that after combustion instability was established, the hydrogen-injection temperature had to be increased to over 30° R (16.7° K) to eliminate instability.

With the available data, it was assumed that chamber length did not affect the system stability appreciably. Essentially all transition temperature data lie within $\pm 4^{\circ}$ R (2.2° K) of a typical instability transition line. The data show no significant stability differences between the various configurations shown on figure 5. From these data, it can be concluded that the various chamber materials tested did not affect stability transition temperature.

Combustion Instability Amplitude

Additional information was obtained from the portion of each test after combustion instability began. Combustion instability amplitudes were compared to determine whether the amplitude is affected by chamber material.

All ablative chamber tests were run with an infinite probe for combustion instability frequency and amplitude sensing. Flush-mounted pickups were used for the steel chamber tests. Therefore, a separate series of tests were run with an infinite probe and several standard flush-mounted pickups mounted near the injector faceplate for comparison. The results of these tests, run with a steel chamber engine are summarized in figure 6. The data points shown in figure 6 were obtained from an analysis of frequency-amplitude plots covering 0.05-second increments during instability. Although this curve indicates a strong tuning of the infinite probe at 6800 hertz, it is relatively flat at the first-tangential mode frequencies of 3300 hertz. This mode was generally predominant

TABLE I. - EXPERIMENTAL DATA

Configuration	Hydrogen injection temperature		Oxidant-fuel ratio, lb/lb (kg/kg)	Exhaust velocity efficiency, percent	Mean-to-peak first-tangential mode instability amplitude								Remarks
					Infinite length probe		Flush-mounted pickup 1		Flush-mounted pickup 2		Average value for each configuration		
	^oR	^oK			psi	kN/m^2	psi	kN/m^2	psi	kN/m^2	psi	kN/m^2	
Uncharred ablative spool (injector 87)	73.6	40.9	4.71	100.6	55.0	379	-----	---	----	---	67.3	464	Transition
	69.5	38.6	3.72	100.3	70.0	482	-----	---	----	---			
	75.7	42.1	5.70	97.8	88.5	610	-----	---	----	---			
	70.9	39.4	4.75	97.6	55.8	384	-----	---	----	---			
Charred ablative spool (injector 86)	70.2	39.0	4.86	94.4	98.8	680	-----	---	----	---	97.1	669	Transition
	69.9	38.8	3.95	96.6	95.2	655	-----	---	----	---			Transition
	78.2	43.5	5.64	97.0	97.3	670	-----	---	----	---			Transition
Steel spool (injector 86)	73.5	40.8	5.02	96.1	----	---	100	689	----	---	101.8	701	Transition
	65.7	36.5	4.11	96.3	----	---	126	868	----	---			
	93.9	52.1	6.00	97.9	----	---	92.0	634	----	---			
	78.1	43.4	5.51	95.4	----	---	89.0	613	----	---			
	72.8	40.5	5.23	88.5	----	---	-----	---	----	---			
Steel spool (injector 87)	62.0	34.4	5.13	98.7	----	---	74.0	510	76.3	525	70.8	488	Unstable
	61.4	34.1	4.93	97.8	----	---	77.5	534	75.5	520			
	78.9	43.8	3.79	97.7	----	---	74.0	510	66.2	456			
	77.3	42.9	3.96	100.3	----	---	60.6	417	62.0	427			
	74.3	41.3	4.99	98.1	----	---	-----	---	----	---			Transition

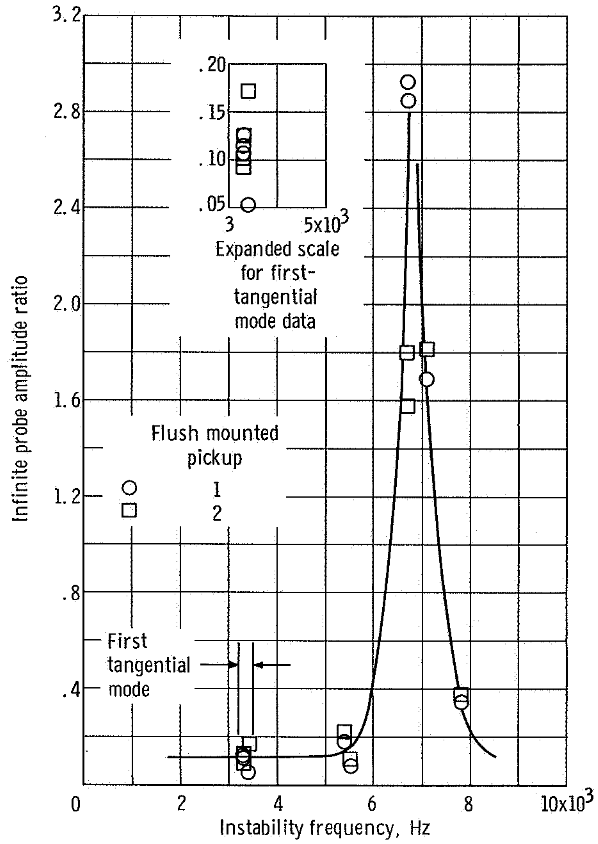

Figure 6. - Calibration of infinite probe.

throughout most of the runs during combustion instability. A secondary mode which was frequently noted at low amplitudes was the combined first-tangential - first-longitudinal at 4100 hertz. The first-tangential mode was used to compare the instability amplitude of the various chambers. The amplitude ratio (amplitude of infinite probe/amplitude of standard pickup) was determined to be 0.111 by averaging all the first-tangential-mode data in figure 6.

The amplitude comparisons of various chambers during unstable operation are summarized in table II. These data were obtained by averaging first-tangential modes, during unstable combustion, on a series of 0.05-second-increment frequency-amplitude plots for each test. Injectors 86 and 87 are identical in design. The average instability amplitude of injector 86 was nearly $1\frac{1}{2}$ times that of injector 87 in the identical steel chamber. However, no significant difference was noted between the uncharred ablative and the steel chamber when tested with injector 87 or the charred ablative and the steel chamber when tested with injector 86. It can then be inferred that there is no difference between charred and uncharred ablative chambers. From these data, it is concluded that there is no significant difference in instability amplitude between the steel, uncharred and charred ablative material chambers.

TABLE II. - FIRST-TANGENTIAL MODE

AMPLITUDE COMPARISONS

Configuration comparisons	Average value amplitude comparisons
Steel chamber with injector 86 to steel chamber with injector 87	1.44
Uncharred ablative chamber with injector 86 to steel chamber with injector 87	.95
Charred ablative chamber with injector 86 to steel chamber with injector 86	.95

SUMMARY OF RESULTS

An investigation was conducted to determine the effect on combustion instability of ablative chambers as compared with steel chambers. The 20 000-pound (89-kN) thrust liquid-hydrogen - liquid-oxygen rocket engine used for this investigation was operated at 300-psia (2070-kN/m^2) chamber pressure. This investigation gave the following results:

1. There was no significant difference in instability transition temperature between the ablative combustion chambers and the steel combustion chamber.

2. Combustion instability amplitude and predominant frequency remained the same for the ablative and the steel combustion chambers.

Lewis Research Center,
National Aeronautics and Space Administration,
Cleveland, Ohio, October 11, 1967,
128-31-06-05-22.

REFERENCES

1. Tomazic, William A.; Conrad, E. William; Godwin, Thomas W.: M-1 Injector Development - Philosophy and Implementation. Paper No. 67-461, AIAA, July 1967.

2. Wanhainen, John P.; Parish, Harold C.; and Conrad, E. William: Effect of Propellant Injection Velocity on Screech in 20,000-Pound Hydrogen-Oxygen Rocket Engine. NASA TN D-3373, 1966.

3. Blackshear, Perry L.; Rayle, Warren D.; and Tower, Leonard K.: Study of Screeching Combustion in a 6-Inch Simulated Afterburner. NACA TN 3567, 1955.

NASA-Langley, 1968 —— 28 E-4099